Surface Stress Effect on the Nonlocal Biaxial Buckling and Bending Analysis of Polymeric Piezoelectric Nanoplate Reinforced by CNT Using Eshelby-Mori-Tanaka Approach

M. Mohammadimehr [1, *], B. Rousta Navi [1], A. Ghorbanpour Arani [2]

[1]*Department of Solid Mechanics ,Faculty of Mechanical Engineering, University of Kashan, Kashan , Iran*
[2]*Institute of Nanoscience & Nanotechnology, University of Kashan, Kashan, Islamic Republic of Iran*

ABSTRACT

In this article, the nonlocal biaxial buckling load and bending analysis of polymeric piezoelectric nanoplate reinforced by carbon nanotube (CNT) considering the surface stress effect is presented. This plate is subjected to electro-magneto-mechanical loadings. Eshelby-Mori-Tanaka approach is used for defining the piezoelectric nanoplate material properties. Navier's type solution is employed to obtain the critical buckling load of polymeric piezoelectric nanoplate for classical plate theory (CPT) and first order shear deformation theory (FSDT). The influences of various parameters on the biaxial nonlocal critical buckling load with respect to the local critical buckling load ratio (λ) of nanoplate are examined. Surface stress effects on the surface biaxial critical buckling load to the non-surface biaxial critical buckling load ratio (γ) can not be neglected. Moreover, the effect of residual surface stress constant on γ is higher than the other surface stress parameters on it. γ increases by applying the external voltage and magnetic fields. The nonlocal deflection to local deflection of piezoelectric nanocomposite plate ratio (η) decreases with an increase in the nonlocal parameter for both theories. And for FSDT, η decreases with an increase in residual stress constant and vice versa for CPT.

© 2015 IAU, Arak Branch.All rights reserved.

Keywords : Polymeric piezoelectric nanoplate; Buckling; Bending; Surface stress effect; Eshelby-Mori-Tanaka approach; SWCNT.

1 INTRODUCTION

NOWADAYS , nano material due to an excellent properties is used to improve the properties of polymeric composite materials in the mechanical and electrical engineering [1, 2]. Nano materials are made in different shapes such as carbon nanotube (CNT) [3], bororn nitride nanotube [4], and etc. CNTs are one of these shapes which are vastly used in many literatures. Also, in composite structures, the CNTs are commonly used as reinforcement particularly in polymeric composites. In the recent decades, the improvements of physicochemical and thermomechanical properties of polymeric composite is the subject of research interest. Polymeric nanocomposites [5] are a new class of materials alternative to usual polymers. In this new class of material, nanosized reinforcements are added in polymer matrix offering wonderful improvement in properties of the

_____
* Corresponding author. Tel.: +98 31 55912423; Fax: +98 31 55912424.
E-mail address: mmohammadimehr@kashanu.ac.ir (M. Mohammadimehr).

polymer. For example, because of exceptional specifications of CNT, properties of polymer composites are enhanced by applying the CNT that is used as nano-particles, nanotubes, nano-fibers, nano-filler, florence and the nanowires [1,2]. Polymeric piezoelectric nanocomposite are used as actuators, transducers, sensor [6] and nanogenerator [7]. This point can be motivated for mechanical and electrical engineering to work in this field.

At the present time, many researchers investigated various parameters on the buckling behavior of nanoplate [8-14]. Their results showed that the critical buckling load decreased by increasing the nonlocal parameter and vice versa with increasing in the thickness of nanoplate. The critical buckling load has more affected by the small scale parameter for uniaxial compression than biaxial compression. As the mode number increases, the nonlocal parameter effect on the buckling load increases. The nonlocal parameter has more effect on nanoplates for length less than 30 nm.

Investigating free vibrations of thin-walled cylindrical shells made of FGPM is crucial in theoretical and practical aspects. To reach a real model, we should consider the interaction of cylindrical shells and surrounded medium with an appropriate model, the Pasternak model is a good choice for this purpose by Pasternak [8].

For the orthotropic single layer graphene sheet (SLGS), many researchers showed that the nonlocal buckling load increases by applied voltage[15] and the difference between the orthotropic and isotropic buckling loads is considerable at the lower nonlocal parameter value [16]. The critical buckling load has more affected by the nonlocal parameter at larger number modes [17].

Many researches have been presented the investigation of surface stress effect on the critical buckling load. Firstly, the theory of surface stress effects is introduced by Gurtin and Murdoch [18]. Two-dimensional finite element formulation of anisotropic material with considering surface effect is established by Tian and Rajapakse [19]. The surface stress effects on the critical buckling load of nanowires is studied by Wang and Feng [20]. They illustrated that the critical buckling load increases with an increase of the positive elastic surface constants. The postbuckling behavior of nanoplates based on classical (CPT) and the Mindlin plate theories is investigated by Wang and co-worker [21]. They showed that the surface stress effect is more significant as the thickness of the plate decreases.

Alzahrani et al. investigated the small scale effect on the bending of graphene sheets under hygro-thermo-mechanical loadings [22]. They showed that the deflection of graphene sheet increases with an increase in moisture and temperature. Alibeigloo studied the bending of composite plate reinforced by functionally graded carbon nanotube embedded in piezoelectric layers using three-dimensional theory of elasticity [23]. They concluded that the displacement decreases with an increase in CNT volume fraction. Furthermore, the effect of the applied voltage on transverse displacement is higher than the other displacement. Zhu et al. extended the finite element method for bending and free vibration analysis of carbon nanotube-reinforced composite plates based on the first order shear deformation (FSDT) [24]. They illustrated that the deflection of nanocomposite plate decreases with an increase of the CNT volume fraction. On the other hands, considering the CNT volume fraction is less than 6%, the deflection of nanocomposite plate reduces more than 30%.

Lei et al. developed the element-free kp-Ritz method for the buckling behavior of composite plate reinforced by functionally graded single-walled carbon nanotube (SWCNT) using FSDT [25]. The biaxial buckling of nanocomposite plate reinforced by SWCNTs using FSDT is studied by Mehrabadi et al. [26]. The Eshelby–Mori–Tanaka approach is employed to obtain the composite material properties. They showed that both uniaxial critical buckling load and biaxial critical buckling load increase with an increase of CNT volume fraction. Also, the uniaxial critical buckling load decreases with a decrease in aspect ratio and vice versa for the biaxial critical buckling load.

In this article, the nonlocal biaxial buckling and bending behavior of polymeric piezoelectric nanocomposite plate subjected to electro-magneto-mechanical loadings is reinforced by CNT based on CPT and FSDT are investigated. Also, the surface stress effect is considered and Eshelby-Mori-Tanaka approach is used to obtain the critical buckling load. Influences of various parameters such as: the nonlocal parameter, surface stress, CNT volume fraction, aspect ratio, applied voltage; magnetic fields and elastic foundation on the buckling behavior of nanoplate are taken into account in this research.

2   GEOMETRY OF POLYMERIC PIEZOELECTRIC NANOCOMPOSITE PLATE

Geometry of polymeric piezoelectric nanoplate reinforced by CNTs is assumed as length a , width b and thickness h respectively. Inner and outer diameters of CNTs are d_i and d_o , respectively. As it can be observed in Fig. 1, the polymeric piezoelectric nanocomposite plate is placed on the elastic medium and subjected to electro-magneto-

mechanical loadings. Also, the cartesian coordinate system placed on the center of the middle-plane of polymeric piezoelectric nanocomposite plate.
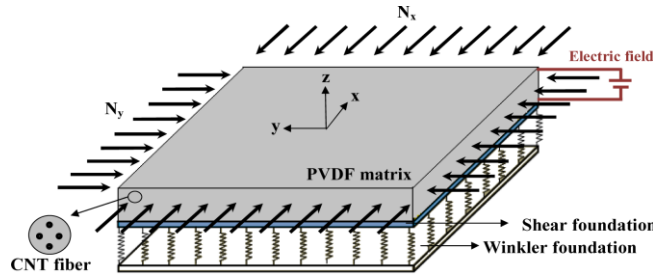

Fig.1
Schematic of polymeric piezoelectric nanoplate reinforced by CNTs under electro-magneto-mechanical loadings.

2.1 Eshelby-Mori-Tanaka approach to obtain the elastic constants

One of the approaches used to obtain the composite material properties is the Eshelby-Mori-Tanaka approach. In this approach, CNT must be straight, long and uniformly distributed in isotropic polymeric piezoelectric nanoplate. Hence the stiffness coefficients of polymeric piezoelectric nanocomposite plate are written as follows [27]:

$$
\begin{aligned}
c_{11} &= \frac{E_m V_m \left(1 + V_f - V_m \upsilon_m\right) + 2V_f V_m \left(k_f n_f - l_f\right)\left(1 + \upsilon_m\right)\left(1 - 2\upsilon_m\right)}{\left(1 + \upsilon_m\right)\left\{2V_m k_f \left(1 - \upsilon_m - 2\upsilon_m^2\right) + E_m \left(1 + V_f - 2\upsilon_m\right)\right\}} + \\
&\quad \frac{E_m \left[2V_m^2 k_f \left(1 - \upsilon_m\right) V_f n_f \left(1 + V_f - 2\upsilon_m\right) - 4V_m l_f \upsilon_m\right]}{2V_m k_f \left(1 - \upsilon_m - 2\upsilon_m^2\right) + E_m \left(1 + V_f - 2\upsilon_m\right)} \\[2mm]
c_{22} &= \frac{E_m \left\{E_m V_m + 2k_f \left(1 + \upsilon_m\right)\left[V_f \left(1 - 2\upsilon_m\right) + 1\right]\right\}}{2\left(1 + \upsilon_m\right)\left\{2V_m k_f \left(1 - \upsilon_m - 2\upsilon_m^2\right) + E_m \left(1 + V_f - 2\upsilon_m\right)\right\}} + \\
&\quad \frac{E_m \left[E_m V_m + 2m_f \left(3 + V_f - 4\upsilon_m\right)\left(1 + \upsilon_m\right)\right]}{2\left(1 + \upsilon_m\right)\left\{E_m \left[V_f + 4V_f \left(1 - \upsilon_m\right)\right] + 2m_f \left(3 + V_f - 4\upsilon_m^2\right)\right\}} \\[2mm]
c_{12} &= \frac{E_m \left\{V_m \upsilon_m \left[E_m + 2k_f \left(1 + \upsilon_m\right)\right] + 2V_f l_f \left(1 - \upsilon_m^2\right)\right\}}{\left(1 + \upsilon_m\right)\left[2Vk \left(1 - \upsilon_m - 2\upsilon_m^2\right) + E_m \left(1 + V - 2\upsilon_m\right)\right]} \\[2mm]
c_{44} &= \frac{E_m \left[E_m V_m + 2m_f \left(3 + V_f - 4\upsilon_m\right)\left(1 + \upsilon_m\right)\right]}{2\left(1 + \upsilon_m\right)\left\{E_m \left[V_m + 4V_f \left(1 - \upsilon_m\right)\right] + 2m_f V_m \left(3 + V_f - 4\upsilon_m^2\right)\right\}} \\[2mm]
c_{55} &= c_{66} = \frac{E_m \left[E_m V_m + 2p_f \left(1 + V_f\right)\left(1 + \upsilon_m\right)\right]}{2\left(1 + \upsilon_m\right)\left[E_m \left(1 + V_f\right) + 2V_m p_f \left(1 + \upsilon_m\right)\right]}
\end{aligned}
\tag{1}
$$

where k_f, n_f, m_f, p_f and υ_m are the Hill's elastic modulli for the CNTs [27] and the Poisson's ratio of matrix.

2.2 Constitutive equations of polymeric piezoelectric nanocomposite plate

In this research, materials of matrix and fiber of polymeric piezoelectric nanocomposite plate are considered PVDF and CNT, respectively. PVDF has a piezoelectric property which easily tolerates applied voltage. In contrast to PVDF, CNTs tolerate magnetic fields.
   Displacement of polymeric piezoelectric nanocomposite plate using FSDT can be expressed as:

$$u(x,y,z) = z\varphi_x$$
$$v(x,y,z) = z\varphi_y$$
$$w(x,y,z) = w(x,y)$$
(2)

where φ_x, φ_y, and w are the rotation about to x, y coordinates and transverse displacement, respectively and it must be noted that for CPT $\varphi_x = -\partial w / \partial x$ and $\varphi_y = -\partial w / \partial y$.

Using Eq. (1), strain-displacement relations according to von Karman kinematic relations are written as:

$$\varepsilon_x = \frac{\partial u}{\partial x} + \frac{1}{2}(\frac{\partial w}{\partial x})^2 = z\frac{\partial \varphi_x}{\partial x} + \frac{1}{2}(\frac{\partial w}{\partial x})^2$$

$$\varepsilon_y = \frac{\partial v}{\partial y} + \frac{1}{2}(\frac{\partial w}{\partial y})^2 = z\frac{\partial \varphi_y}{\partial y} + \frac{1}{2}(\frac{\partial w}{\partial y})^2$$

$$\varepsilon_z = \frac{\partial w}{\partial x} = 0$$
(3)

$$\gamma_{xy} = \frac{\partial v}{\partial x} + \frac{\partial u}{\partial y} + \frac{\partial w}{\partial x}\frac{\partial w}{\partial y} = z\left(\frac{\partial \varphi_x}{\partial y} + \frac{\partial \varphi_y}{\partial x}\right) + \frac{\partial w}{\partial x}\frac{\partial w}{\partial y}$$

$$\gamma_{xz} = \frac{\partial u}{\partial z} + \frac{\partial w}{\partial x} = \varphi_x + \frac{\partial w}{\partial x}$$

$$\gamma_{yz} = \frac{\partial v}{\partial z} + \frac{\partial w}{\partial y} = \varphi_y + \frac{\partial w}{\partial y}$$

In classical or local theory of continuum mechanics, the stress at a point is only proportional to the strain at that point. This theory is valid for large scale. In small scale, the stress at a reference point x is a function of the strain at all the other points of the body. This phenomenon is known as small-scale effect which is cleared in constitutive equations by the parameter $e_0 a$ and its theory is identified as small-scale or non-local theory. For a structure in the nanoscale, it is not reasonable to ignore the small-scale effect ($e_0 a$). By ignoring this term ($e_0 a = 0$), the non-local theory reduces to local or classical theory which have no desired accuracy for the analysis of CNTs. The constitutive equations of non-local theory for polymeric piezoelectric nanocomposite plate can be written as follows [28, 29]:

$$(1 - (e_0 a)^2 \nabla^2)\begin{Bmatrix} \sigma_x \\ \sigma_y \\ \sigma_{yz} \\ \sigma_{xz} \\ \sigma_{xy} \end{Bmatrix} = \begin{bmatrix} c_{11} & c_{12} & 0 & 0 & 0 \\ c_{12} & c_{22} & 0 & 0 & 0 \\ 0 & 0 & c_{44} & 0 & 0 \\ 0 & 0 & 0 & c_{55} & 0 \\ 0 & 0 & 0 & 0 & c_{66} \end{bmatrix}\begin{Bmatrix} \varepsilon_x \\ \varepsilon_y \\ \gamma_{yz} \\ \gamma_{xz} \\ \gamma_{xy} \end{Bmatrix} - \begin{bmatrix} 0 & 0 & e_{31} \\ 0 & 0 & e_{32} \\ 0 & e_{24} & 0 \\ e_{15} & 0 & 0 \\ 0 & 0 & 0 \end{bmatrix}\begin{Bmatrix} E_x \\ E_y \\ E_z \end{Bmatrix}$$

(4)

$$\begin{Bmatrix} D_x \\ D_y \\ D_z \end{Bmatrix} = \begin{bmatrix} 0 & 0 & 0 & e_{15} & 0 \\ 0 & 0 & e_{24} & 0 & 0 \\ e_{31} & e_{32} & 0 & 0 & 0 \end{bmatrix}\begin{Bmatrix} \varepsilon_x \\ \varepsilon_y \\ \gamma_{yz} \\ \gamma_{xz} \\ \gamma_{xy} \end{Bmatrix} + \begin{bmatrix} \zeta_{11} & 0 & 0 \\ 0 & \zeta_{22} & 0 \\ 0 & 0 & \zeta_{33} \end{bmatrix}\begin{Bmatrix} E_x \\ E_y \\ E_z \end{Bmatrix}$$

where c_{ij}, e_{ij} and ζ_{ii} denote stiffness, piezoelectric and dielectric constants, respectively. $\sigma_{ij}, \varepsilon_{ij}, D_i$ and E_i are stress, electrical displacement, strain components and electric field, respectively.

The electric field can be expressed as the electric potential ϕ:

$$E = -\nabla \phi$$
(5)

The electric potential ϕ must satisfy Maxwell's relation, thus it is considered as [21, 26]:

$$\phi(x,y,z,t) = -\cos(\pi z / h)\phi(x,y,t) + 2zV_0 e^{i\omega t} / h \tag{6}$$

where $\phi(x,y,t)$ and V_0 are the electric potential function and the applied voltage. The natural frequency of the polymeric piezoelectric nanocomposite plate, ω is zero for buckling:

2.3 Derivation of the governing equations

With considering the surface effect, Hamilton's principle yields [28]:

$$\int \left(\delta W_{ext} - \delta U - \delta U^s \right) dt = 0 \tag{7}$$

where $\delta U, \delta U^s$ and δW_{ext} are variations of strain energy, the surface energy, and the external work, respectively.
Variation of strain energy is expressed as:

$$\delta U = \int_V \left(\sigma_x \delta \varepsilon_x + \sigma_y \delta \varepsilon_y + \sigma_{xy} \delta \varepsilon_{xy} - D_x \delta E_x - D_y \delta E_y - D_z \delta E_z \right) dV \tag{8}$$

Substituting Eqs. (3), (5), (6) into Eq. (8) and simplifying it, the subsequent expressions are achieved as:

$$\delta U = -\int_A \left\{ \begin{array}{l} M_{x,x}\delta\varphi_x + \dfrac{\partial}{\partial x}(N_x \dfrac{\partial w}{\partial x})\delta w + M_{y,y}\delta\varphi_y + \dfrac{\partial}{\partial y}(N_y \dfrac{\partial w}{\partial y})\delta w \\[2mm] +M_{xy,y}\delta\varphi_x + M_{xy,x}\delta\varphi_y + \dfrac{\partial}{\partial x}(N_{xy}\dfrac{\partial w}{\partial y})\delta w + \dfrac{\partial}{\partial y}(N_{xy}\dfrac{\partial w}{\partial x})\delta w - N_{xz}\delta\varphi_x - N_{xz,x}\,\delta w - N_{yz}\delta\varphi_y + \\[2mm] N_{yz,y}\,\delta w + \dfrac{\partial}{\partial x}\left(D_x \cos(\dfrac{\pi z}{h})\right)\delta\phi + \dfrac{\partial}{\partial y}\left(D_y \cos(\dfrac{\pi z}{h})\right)\delta\phi + D_z \dfrac{\pi}{h}\sin(\dfrac{\pi z}{h})\delta\phi \end{array} \right\} dA \tag{9}$$

In Eq. (9), the boundary condition expressions are disregarded. The resultant forces (N_{ij}), resultant moments (M_{ij}) and in-plane critical buckling loads ($N_x^{cr}, N_y^{cr}, N_{xy}^{cr}$) can be determined as:

$$\begin{Bmatrix} N_x \\ N_y \\ N_{xy} \\ N_{xz} \\ N_{yz} \end{Bmatrix} = \int_{-h/2}^{h/2} \begin{Bmatrix} \sigma_x \\ \sigma_y \\ \sigma_{xy} \\ k\sigma_{xz} \\ k\sigma_{yz} \end{Bmatrix} dz, \qquad \begin{Bmatrix} M_x \\ M_y \\ M_{xy} \end{Bmatrix} = \int_{-h/2}^{h/2} \begin{Bmatrix} \sigma_x \\ \sigma_y \\ \tau_{xy} \end{Bmatrix} z\,dz \tag{10}$$

$$\begin{aligned} N_x^{cr} &= N_x^{mechan} + N_x^{elect} \quad , N_x^{elect} = 2\,e_{13}\,V_0 \\ N_y^{cr} &= N_y^{mechan} + N_y^{elect}, \; N_y^{elect} = 2\,e_{23}\,V, \; N_y^{mechan} = \alpha N_x^{mechan}, N_{xy}^{cr} = 0 \end{aligned} \tag{11}$$

where k is the shear correction factor which is used in FSDT and equal to 5/6.
Surface stress components considering linear change of *z* stress component are expressed as following equations [30].

$$\sigma_x^s = \frac{2\upsilon z}{h(1-\upsilon)}\left(\tau_s\frac{\partial^2 w}{\partial x^2} + \tau_s\frac{\partial^2 w}{\partial y^2}\right) + E_s\varepsilon_x + \tau_s$$

$$\sigma_y^s = \frac{2\upsilon z}{h(1-\upsilon)}\left(\tau_s\frac{\partial^2 w}{\partial x^2} + \tau_s\frac{\partial^2 w}{\partial y^2}\right) + E_s\varepsilon_x + \tau_s$$

$$\sigma_{xz}^s = \tau_s\frac{\partial w}{\partial x}$$

$$\sigma_{yz}^s = \tau_s\frac{\partial w}{\partial y}$$

(12)

where τ_s and E_s are the residual stress constant and surface Lame constant, respectively.

Variation of surface energy can be written as:

$$\delta U^s = \int_A \left(\sigma_x^s\delta\varepsilon_x + \sigma_y^s\delta\varepsilon_y + \sigma_{xz}^s\delta\varepsilon_{xz} + \sigma_{yz}^s\delta\varepsilon_{yz}\right)dA$$

(13)

Substituting Eqs. (4) and (12) into Eq. (13) and ignoring the nonlinear expressions, the following terms are obtained: for nanopiezoplate (matrix) is considered as:

$$
\begin{aligned}
\delta U^s = & -\frac{\upsilon\tau_s h^2}{6(1-\upsilon)}\left(\frac{\partial^3 w}{\partial x^3} + \frac{\partial^3 w}{\partial x\partial y^2}\right)\delta\varphi_x - \frac{\upsilon\tau_s h^2}{6(1-\upsilon)}\left(\frac{\partial^3 w}{\partial y^3} + \frac{\partial^3 w}{\partial y\partial x^2}\right)\delta\varphi_y - \\
& \frac{\upsilon\tau_s h^2}{6(1-\upsilon)}\nabla^4 w\delta w + \frac{\upsilon\rho_s h^2}{6(1-\upsilon)}\left(\frac{\partial^3 w}{\partial t^2\partial x}\delta\varphi_x + \frac{\partial^3 w}{\partial t^2\partial y}\delta\varphi_y\right) - \\
& 4\tau_s(b+h)\left(\frac{\partial^2 w}{\partial x^2} + \frac{\partial^2 w}{\partial y^2}\right)\delta w + \frac{\upsilon\rho_s h^2}{6(1-\upsilon)}\left(\frac{\partial^4 w}{\partial t^2\partial x^2} + \frac{\partial^4 w}{\partial t^2\partial y^2}\right)\delta w \\
& E_s(bh^2/2 + h^3/6)\left(\frac{\partial^2\varphi_x}{\partial x^2}\delta\varphi_x + \frac{\partial^2\varphi_y}{\partial y^2}\delta\varphi_y\right) + \\
& 2\tau_s(b+h)\left(\frac{\partial w}{\partial x}\delta\varphi_x + \frac{\partial w}{\partial y}\delta\varphi_y\right)
\end{aligned}
$$

(14)

For carbon nanotubes (fibers) [31].

$$\delta U_{cnt}^s = 4\tau_{s\,cnt}d\left(\frac{\partial^2 w}{\partial x^2} + \frac{\partial^2 w}{\partial y^2}\right)\delta w - E_{s\,cnt}(3\pi d^3/8)\left(\frac{\partial^2\varphi_x}{\partial x^2}\delta\varphi_x + \frac{\partial^2\varphi_y}{\partial y^2}\delta\varphi_y\right)$$

(15)

The electro-dynamic Maxwell relations and variation of external work done by magnetic fields for the polymeric piezoelectric nanocomposite plate can be expressed as [32].

$$\vec{h} = \nabla\times\left(\vec{U}\times\vec{H}\right)$$

$$\vec{J} = \nabla\times\vec{h}$$

$$\vec{f_l} = \eta\left(\vec{J}\times H\right)$$

$$\delta W_{ext}^{f_l} = \int_V \left(f_{xl}\delta u + f_{yl}\delta v + f_{zl}\delta w\right)dV$$

(16)

where $\vec{H}, \vec{h}, \vec{U}, \vec{J}, \vec{f_l} \eta$ and $\delta W_{ext}^{f_l}$ are magnetic intensity vector, perturbation of magnetic field vector, displacement vector, electric current density vector, Lorentz force, magnetic permeability and the external work variation, respectively.

Substituting Eq. (2) into Eq. (16) yields for magnetic intensity vector in z direction $(0, 0, H_z)$:

$$\delta W_{ext}^{fl} = \int_A \frac{\eta h^3}{12} H_z^2 \left(\left(\frac{\partial^2 \varphi_x}{\partial x^2} + \frac{\partial^2 \varphi_y}{\partial x \partial y} \right) \delta \varphi_x + \left(\frac{\partial^2 \varphi_y}{\partial y^2} + \frac{\partial^2 \varphi_x}{\partial x \partial y} \right) \delta \varphi_y \right) dA \tag{17}$$

Correspondingly, variation of the external work for magnetic intensity vector in *y* direction:

$$\delta W_{ext}^{f_l} = \int_V \left(f_{xl} \delta u + f_{zl} \delta w \right) dV = \int_A \left(\left(\frac{\partial^2 \varphi_x}{\partial x^2} + \frac{\partial^2 \varphi_x}{\partial y^2} \right) \frac{h^3}{12} \delta \varphi_x + \left(\frac{\partial^2 w}{\partial y^2} + \frac{\partial \varphi_x}{\partial x} \right) h \delta w \right) \eta H_y^2 \ dA \tag{18}$$

Variations of work done by the elastic foundation and transverse force can be written as [32]:

$$\delta W_{ext}^{f_p} = \int_A \left(f_w \delta w + f_g \delta w + q \delta w \right) dA = \int_A \left(k_w w \delta w - k_g \nabla^2 w \delta w + q \delta w \right) dA \tag{19}$$

where k_g, k_w, and *q* are Pasternak shear, Winkler spring parameters and transverse force ,respectively.

Using Eqs. (9), (14), (15), (17) and (19), the governing equations of biaxial buckling load for polymeric piezoelectric nanoplate with surface stress effect are obtained as:

For CPT:

$$M_{x,xx} + 2M_{xy,xy} + M_{y,yy} + \frac{\partial}{\partial x}((N_x^{mechan} + N_x^{elect}) \frac{\partial w}{\partial x}) + \frac{\partial}{\partial y}(N_y \frac{\partial w}{\partial y}) + \frac{\partial}{\partial x}(N_{xy} \frac{\partial w}{\partial y}) +$$

$$\frac{\partial}{\partial x}(N_{xy} \frac{\partial w}{\partial y}) - \frac{\upsilon h^2 \tau_s}{6(1-\upsilon)} \nabla^4 w - E_s (bh^2/2 + h^3/6) \left(\frac{\partial^4 w}{\partial x^4} + \frac{\partial^4 w}{\partial y^4} \right) - 2\tau_{scnt}(d_i + d_o) \left(\frac{\partial^2 w}{\partial x^2} + \frac{\partial^2 w}{\partial y^2} \right) +$$

$$E_{scnt}(3\pi(d_i^3 + d_o^3)/8) \left(\frac{\partial^4 w}{\partial x^4} + \frac{\partial^4 w}{\partial y^4} \right) + 2\tau_s(b+h) \left(\frac{\partial^2 w}{\partial x^2} + \frac{\partial^2 w}{\partial y^2} \right) + k_w w - k_g \nabla^2 w + f_{zl} = 0 \tag{20}$$

$$\frac{\partial}{\partial x} \left(D_x \cos(\frac{\pi z}{h}) \right) + \frac{\partial}{\partial y} \left(D_y \cos(\frac{\pi z}{h}) \right) + D_z \frac{\pi}{h} \sin(\frac{\pi z}{h}) = 0$$

For FSDT:

$$M_{x,x} + M_{xy,y} - N_{xz} + \frac{\upsilon h^2 \tau_s}{6(1-\upsilon)} \left(\frac{\partial^3 w}{\partial x^3} + \frac{\partial^3 w}{\partial x \partial y^2} \right) + E_s(bh^2/2 + h^3/6) \frac{\partial^2 \varphi_x}{\partial x^2} - 2\tau_s(b+h) \frac{\partial w}{\partial x} +$$

$$E_{scnt}(3\pi(d_i^3 + d_o^3)/8) \frac{\partial^2 \varphi_x}{\partial x^2} + f_x^l = 0$$

$$M_{y,y} + M_{xy,x} - N_{yz} - \frac{\upsilon h^2 \tau_s}{6(1-\upsilon)} \left(\frac{\partial^3 w}{\partial y^3} + \frac{\partial^3 w}{\partial y \partial x^2} \right) + E_s(bh^2/2 + h^3/6) \frac{\partial^2 \varphi_y}{\partial y^2} - 2\tau_s(b+h) \frac{\partial w}{\partial y} + \tag{21}$$

$$E_{scnt}(3\pi(d_i^3 + d_o^3)/8) \frac{\partial^2 \varphi_y}{\partial y^2} + f_y^l = 0$$

$$N_{yz,y} + N_{xz,x} + 4\tau_s(b+h) \left(\frac{\partial^2 w}{\partial x^2} + \frac{\partial^2 w}{\partial y^2} \right) + k_w w - k_g \nabla^2 w + f_z^l - 4\tau_{scnt}(d_i + d_o) \left(\frac{\partial^2 w}{\partial x^2} + \frac{\partial^2 w}{\partial y^2} \right) = 0$$

$$\int_{-h/2}^{h/2} \left(\cos \left(\frac{\pi z}{h} \right) \left(\frac{\partial D_x}{\partial x} \right) \delta \phi + \cos \left(\frac{\pi z}{h} \right) \frac{\partial D_y}{\partial y} \delta \phi + \frac{\pi}{h} \sin \left(\frac{\pi z}{h} \right) D_z \delta \phi \right) dz = 0$$

2.4 The nonlocal governing equations of polymeric piezoelectric nanocomposite plate

Using nonlocal piezoelasticity theory [33] and substituting Eqs. (4) and (9) into Eqs. (20) and (21), the nonlocal governing equations of the biaxial buckling load for polymeric piezoelectric nanocomposite plate can be obtained as:

For CPT:

$$
-\frac{h^3}{12}\left(c_{11}\frac{\partial^4 w}{\partial x^4}+2c_{12}\frac{\partial^4 w}{\partial y^2 \partial x^2}+4c_{66}\frac{\partial^4 w}{\partial y^2 \partial x^2}+c_{22}\frac{\partial^4 w}{\partial y^4}\right)+(1-(e_0a)^2\nabla^2)\left[\frac{\partial}{\partial x}((N_x^{mechan}+N_x^{elect})\frac{\partial w}{\partial x})+\frac{\partial}{\partial y}(N_y\frac{\partial w}{\partial y})\right]+
$$

$$
(1-(e_0a)^2\nabla^2)\left[\frac{\partial}{\partial x}(N_{xy}\frac{\partial w}{\partial y})+\frac{\partial}{\partial x}(N_{xy}\frac{\partial w}{\partial y})\right]+\frac{\upsilon h^2 \tau_s}{6(1-\upsilon)}\nabla^4 w-(1-(e_0a)^2\nabla^2)\left[E_s(bh^2/2+h^3/6)\left(\frac{\partial^4 w}{\partial x^4}+\frac{\partial^4 w}{\partial y^4}\right)\right]-
$$

$$
(1-(e_0a)^2\nabla^2)\left[2\tau_s(b+h)\left(\frac{\partial^2 w}{\partial x^2}+\frac{\partial^2 w}{\partial y^2}\right)+2\tau_{scnt}\left(d_i+d_o\right)\left(\frac{\partial^2 w}{\partial x^2}+\frac{\partial^2 w}{\partial y^2}\right)\right]-E_{scnt}(3\pi\left(d_i^3+d_o^3\right)/8)\left(\frac{\partial^4 w}{\partial x^4}+\frac{\partial^4 w}{\partial y^4}\right)+
$$

$$
(1-(e_0a)^2\nabla^2)\left[-k_w w+k_g\nabla^2 w+f_{zl}-q(x,y)\right]+\left(\frac{2e_{31}h}{\pi}\phi_{,xx}+\frac{2e_{32}h}{\pi}\phi_{,yy}\right)=0
$$

$$
(1-(e_0a)^2\nabla^2)\left[\xi_{11}\frac{h}{2}\phi_{,xx}+\xi_{22}\frac{h}{2}\phi_{,yy}-2e_{31}\frac{h}{\pi}\frac{\partial^2 w}{\partial x^2}-2e_{32}\frac{h}{\pi}\frac{\partial^2 w}{\partial y^2}-\frac{h}{2}\xi_{33}\phi\right]=0
$$

(22)

For FSDT:

$$
\frac{C_{11}h^3}{12}\varphi_{x,xx}+\frac{C_{12}h^3}{12}\varphi_{y,xy}+d_5\phi_x+\frac{C_{66}h^3}{12}\varphi_{x,yy}+\frac{C_{66}h^3}{12}\varphi_{y,xy}-C_{55}hw_{,x}-C_{55}h\varphi_x+d_1\phi_{,x}+\frac{\upsilon h^2\tau_s}{6(1-\upsilon)}\left(\frac{\partial^3 w}{\partial x^3}+\frac{\partial^3 w}{\partial x\partial y^2}\right)+
$$

$$
(1-(e_0a)^2\nabla^2)E_s(bh^2/2+h^3/6)\frac{\partial^2\varphi_x}{\partial x^2}-2\tau_s(1-(e_0a)^2\nabla^2)(b+h)\frac{\partial w}{\partial x}+E_{scnt}(3\pi\left(d_i^3+d_o^3\right)/8)\frac{\partial^2\varphi_x}{\partial x^2}+(1-(e_0a)^2\nabla^2)f_x^l=0
$$

$$
\frac{C_{12}h^3}{12}\varphi_{x,xy}+\frac{C_{22}h^3}{12}\varphi_{y,yy}+d_6\phi_{,y}+\frac{C_{66}h^3}{12}\varphi_{x,xy}+\frac{C_{66}h^3}{12}\varphi_{y,xx}-C_{44}hw_{,y}-C_{44}h\varphi_y+d_3\phi_{,y}+\frac{\upsilon h^2\tau_s}{6(1-\upsilon)}\left(\frac{\partial^3 w}{\partial y^3}+\frac{\partial^3 w}{\partial y\partial x^2}\right)+
$$

$$
(1-(e_0a)^2\nabla^2)E_s(bh^2/2+h^3/6)\frac{\partial^2\varphi_y}{\partial y^2}-2\tau_s(1-(e_0a)^2\nabla^2)(b+h)\frac{\partial w}{\partial y}+E_{scnt}(3\pi\left(d_i^3+d_o^3\right)/8)\frac{\partial^2\varphi_y}{\partial y^2}+(1-(e_0a)^2\nabla^2)f_y^l=0
$$

(23)

$$
C_{44}hw_{,yy}+C_{44}h\varphi_{y,y}+d_3\phi_{,yy}+C_{55}hw_{,xx}+C_{55}h\varphi_{x,x}+d_1\phi_{,xx}+4\tau_s(1-(e_0a)^2\nabla^2)(b+h)\left(\frac{\partial^2 w}{\partial x^2}+\frac{\partial^2 w}{\partial y^2}\right)+
$$

$$
k_w(1-(e_0a)^2\nabla^2)w-q(x,y)-k_g(1-(e_0a)^2\nabla^2)\nabla^2 w+(1-(e_0a)^2\nabla^2)f_z^l-4\tau_{scnt}(1-(e_0a)^2\nabla^2)\left(d_i+d_o\right)\left(\frac{\partial^2 w}{\partial x^2}+\frac{\partial^2 w}{\partial y^2}\right)=0
$$

$$
(1-(e_0a)^2\nabla^2)\left[d_1\varphi_{x,x}+d_1w_{,xx}+d_2\phi_{,xx}+d_3\varphi_{y,y}+d_3w_{,yy}+d_4\phi_{,yy}+d_5\varphi_{x,x}+d_6\varphi_{y,y}-d_7\phi\right]=0
$$

where:

$$
d_1=\int_{-h/2}^{h/2}e_{15}\cos\left(\frac{\pi z}{h}\right)dz,\ d_2=\int_{-h/2}^{h/2}\xi_{11}\cos^2\left(\frac{\pi z}{h}\right)dz,\ d_3=\int_{-h/2}^{h/2}e_{24}\cos\left(\frac{\pi z}{h}\right)dz,
$$

$$
d_4=\int_{-h/2}^{h/2}\xi_{22}\cos^2\left(\frac{\pi z}{h}\right)dz,\ d_5=\int_{-h/2}^{h/2}\frac{\pi e_{31}}{h}z\sin\left(\frac{\pi z}{h}\right)dz,\ d_6=\int_{-h/2}^{h/2}\frac{\pi e_{32}}{h}z\sin\left(\frac{\pi z}{h}\right)dz,
$$

$$
d_7=\int_{-h/2}^{h/2}\xi_{33}\left(\frac{\pi}{h}\right)^2\sin^2\left(\frac{\pi z}{h}\right)dz
$$

(24)

3   NAVIER's TYPE SOLUTION OF THE NONLOCAL BIAXIAL CRITICAL BUCKLING LOAD

Navier's type solution for the nonlocal biaxial critical buckling load of polymeric piezoelectric nanocomposite plate reinforced by CNT can be defined as:

$$w(x,y) = \sum_{i=1}^{m}\sum_{j=1}^{n} w_{mn}\sin(m\pi x/a)\sin(n\pi y/b)$$

$$\varphi_x(x,y) = \sum_{i=1}^{m}\sum_{j=1}^{n} \varphi_{xmn}\cos(m\pi x/a)\sin(n\pi y/b)$$

$$\varphi_y(x,y) = \sum_{i=1}^{m}\sum_{j=1}^{n} \phi_{ymn}\sin(m\pi x/a)\cos(n\pi y/b)$$

$$\phi(x,y) = \sum_{i=1}^{m}\sum_{j=1}^{n} \phi_{mn}\sin(m\pi x/a)\sin(n\pi y/b) \qquad (25)$$

$$q(x,y) = \sum_{i=1}^{m}\sum_{j=1}^{n} q_{mn}\sin(m\pi x/a)\sin(n\pi y/b)$$

$$q_{mn} = \frac{4}{ab}\int_0^a\int_0^b q(x,y)\sin(m\pi x/a)\sin(n\pi y/b)\,dy\,dx$$

where n and m are the transverse and axial wave numbers, respectively.

Substituting Eq. (25) into Eqs. (22) and (23), the governing equations can be expressed as following matrix form:

For CPT:

$$\begin{bmatrix} A+BN^{cr} & C \\ D & E \end{bmatrix}\begin{Bmatrix} w_{mn} \\ \phi_{mn} \end{Bmatrix} = \begin{Bmatrix} 0 \\ 0 \end{Bmatrix} \qquad (26)$$

where

$$\alpha_1 = \frac{m\pi}{a} \qquad\qquad \alpha_2 = \frac{n\pi}{b}$$

$$B = \left(\alpha_1^2 + \alpha\alpha_2^2\right) \qquad\qquad \beta = (1 + \mu^2(\alpha_1^2 + \alpha_2^2))$$

$$A = \left(-\frac{h^3}{12}\left[\begin{array}{l}\left(c_{11} + E_{scnt}(3\pi(d_i^3 + d_o^3)/8)\right)\alpha_1^4 + (2c_{12} + 4c_{66})\alpha_1^2\alpha_2^2 + \\ \left(c_{22} + E_{scnt}(3\pi(d_i^3 + d_o^3)/8)\right)\alpha_2^4\end{array}\right]\right) +$$

$$\frac{\upsilon h^2\tau_s}{6(1-\upsilon)}(\alpha_1^2 + \alpha_2^2)^2 - \beta\left(E_s(bh^2/2 + h^3/6)\right)(\alpha_1^4 + \alpha_2^4) + \qquad (27)$$

$$\beta\left[2\tau_s(b+h) + 2\tau_{scnt}(d_i + d_o)\right](\alpha_1^2 + \alpha_2^2) - \beta k_w + \beta k_g(\alpha_1^2 + \alpha_2^2) + \beta f_{lz} - 2\lambda_1^2 e_{13}V_0\beta - 2\lambda_2^2 e_{23}V_0\beta + \beta q$$

$$C = \left(-\frac{2e_{31}h}{\pi}\alpha_1^2 - \frac{2e_{32}h}{\pi}\alpha_2^2\right)$$

$$D = 2e_{31}\frac{h}{\pi}\alpha_1^2 + 2\alpha_2^2 e_{32}\frac{h}{\pi}$$

$$E = -\xi_{11}\alpha_1^2\frac{h}{2} - \xi_{22}\alpha_2^2\frac{h}{2} - \frac{h}{2}\xi_{33}$$

For FSDT:

$$\begin{bmatrix} F+\beta BN_x^{cr} & G & H & I \\ J & L & M & N \\ P & Q & R & S \\ T & V & W & X \end{bmatrix} \begin{Bmatrix} w_{mn} \\ \varphi_{xmn} \\ \varphi_{ymn} \\ \phi_{mn} \end{Bmatrix} = 0 \tag{28}$$

where:

$$F = -C_{44}h\alpha_2^2 - \alpha_1^2 C_{55}h - 4\tau_s\beta(b+h)\left(\alpha_2^2 + \alpha_1^2\right) + k_w\beta + \beta k_g + 4\tau_{scnt}\beta\left(\alpha_1^2 + \alpha_2^2\right)(d_i + d_o) - 2\alpha_1^2 e_{13}V_0\beta -$$
$$\beta\left(\eta h H_y^2 \alpha_2^2 + \eta h H_x^2 \alpha_1^2\right) - 2\alpha_2^2 e_{23}V_0\beta$$

$$G = -C_{55}h\alpha_1$$

$$H = -C_{44}h\alpha_2$$

$$I = -d_1\alpha_1^2 - d_3\alpha_2^2$$

$$J = -C_{55}h\,\alpha_1 - \frac{\upsilon h^2 \tau_s}{6(1-\upsilon)}\left(\alpha_1^3 + \alpha_1\alpha_2^2\right) + 2\tau_s\beta(b+h)\alpha_1$$

$$L = -\frac{C_{11}h^3}{12}\alpha_1^2 - \frac{C_{66}h^3}{12}\alpha_2^2 - C_{55}h - E_s\beta(bh^2/2 + h^3/6)\alpha_1^2 -$$
$$E_{scnt}(3\pi\left(d_i^3 + d_o^3\right)/8)\alpha_1^2 - \beta\left(\alpha_1^2 + \alpha_2^2\right)\frac{\eta h^3}{12}H_y^2 - \beta\frac{\eta h^3}{12}H_z^2\alpha_1^2$$

$$M = \left(-\frac{C_{12}h^3}{12} - \frac{C_{66}h^3}{12} + \beta\left(\frac{\eta h^3}{12}H_z^2\right)\right)\alpha_1\alpha_2$$

$$N = \left(d_5 - d_1\right)\alpha_1 \tag{29}$$

$$P = -C_{44}h\alpha_2 - \frac{\upsilon h^2 \tau_s}{6(1-\upsilon)}\left(\alpha_2^3 + \alpha_2\alpha_1^2\right) + 2\tau_s\beta(b+h)\alpha_2 - \beta\eta h H_y^2 \alpha_1 - C_{55}h\alpha_1$$

$$Q = \left(-\frac{C_{12}h^3}{12} - \frac{C_{66}h^3}{12}\right)\alpha_1\alpha_2 - \beta\eta h H_x^2 \alpha_2$$

$$R = -\frac{C_{22}h^3}{12}\alpha_2^2 - \frac{C_{66}h^3}{12}\alpha_1^2 - C_{44}h - \beta E_s(bh^2/2 + h^3/6)\alpha_2^2 -$$
$$E_{scnt}(3\pi\left(d_i^3 + d_o^3\right)/8)\alpha_2^2 - \beta\frac{\eta h^3}{12}H_z^2\alpha_2^2 - \beta\left(\alpha_1^2 + \alpha_2^2\right)\frac{\eta h^3}{12}H_x^2$$

$$S = -\left(d_3 + d_6\right)\alpha_2$$

$$T = -d_3\alpha_2^2 - d_1\alpha_1^2$$

$$V = -\left(d_1 + d_5\right)\alpha_1$$

$$W = -\left(d_3 + d_6\right)\alpha_2$$

$$X = -d_2\alpha_1^2 - d_4\alpha_2^2 - d_7$$

It is noted that the determinant of Eq. (23) should be equal to zero. Then the nonlocal critical biaxial buckling load can be obtained as:

For CPT:

$$N_x^{cr} = \frac{(DC/E) - A}{(1 + \mu^2(\alpha_1^2 + \alpha_2^2))B} \tag{30}$$

For FSDT:

$$N_x^{cr} = \left[\left(\left(G \det(k_2) - H \det(k_3) + I \det(k_4) \right) / \det(k_1) \right) - F \right] / \beta B \tag{31}$$

where:

$$k_1 = \begin{bmatrix} L & M & N \\ Q & R & S \\ V & W & X \end{bmatrix}, \quad k_2 = \begin{bmatrix} J & M & N \\ P & R & S \\ T & W & X \end{bmatrix}$$

$$k_3 = \begin{bmatrix} J & L & N \\ P & Q & S \\ T & V & X \end{bmatrix}, \quad k_4 = \begin{bmatrix} J & L & M \\ P & Q & R \\ T & V & W \end{bmatrix} \tag{32}$$

3.1 The deflection of polymeric piezoelectric nanoplate reinforced by CNT

By eliminating the critical buckling loads in Eqs. (22) and (23), the deflection of polymeric piezoelectric nanoplate reinforced by CNT is obtained for CPT and FSDT as following form:
For CPT:

$$w_{mn} = \frac{q_{mn}}{A - (CD / E)} \tag{33}$$

For FSDT:

$$w_{mn} = \frac{q_{mn}}{F + G\left(a_{11} - a_{13}a_{10} / a_{12}\right) + H\left(a_{14} - a_{13}a_{15} / a_{12}\right) + I\left(a_{13} / a_{12}\right)} \tag{34}$$

where:

$$a_1 = \frac{M}{L}, a_2 = \frac{N}{L}, a_3 = \frac{J}{L}, a_4 = R - \frac{MQ}{L}, a_5 = S - \frac{NQ}{L}, a_6 = P - \frac{JQ}{L},$$

$$a_7 = W - \frac{MV}{L}, a_8 = X - \frac{NV}{L}, a_9 = T - \frac{JV}{L}, a_{10} = a_2 - \frac{a_1 a_5}{a_4}, \tag{35}$$

$$a_{11} = a_3 - \frac{a_1 a_6}{a_4}, a_{12} = a_8 - \frac{a_7 a_5}{a_4}, a_{13} = a_9 - \frac{a_6 a_7}{a_4}, a_{14} = \frac{a_6}{a_4}, a_{15} = \frac{a_5}{a_4}$$

4   RESULTS AND DISCUSSION

In this article, the biaxial critical buckling load of nonlocal polymeric piezoelectric nanocomposite plate reinforced by CNT using Eshelby-Mori-Tanaka approach are studied. Effects of various parameters such as the volume fraction of CNT, aspect ratio, spring and shear constants of the elastic foundation, the nonlocal parameter, surface stress, the applied voltage and magnetic fields on the biaxial critical buckling load of piezoelectric nanocomposite plate are investigated.

The material properties, CNTs, and plate dimensions, surface stress parameters for CNTs and nanoplate, elastic coefficients, magnetic field intensity and applied voltage are listed in Table 1. [34]

The nonlocal uniaxial and biaxial critical buckling load ratios ($N^{cr} = 12(1-v^2)N_x^{cr}L^2 / c_{11}h^3$) of nanoplate for the present work are computed that this results have been listed in Table 2. Comparison between the analytical results of the present work and the obtained analytical results by Murmu et al. [13] has a good agreement between them.

Table 1
Material properties, geometry dimensions, elastic foundation parameter and values of external field [34]

parameter	polystyren	PVDF	CNT
E	1.9 GPa	2.5 GPa	
v	0.3	0.3	0.175
V_f			0.14
τ_s		1.7 N/m	0.9108 N/m
E_s		4 N/m	5.1882 N/m
$e_0 a$		0.5nm	0.5nm
a	25mm	9.26nm	
b	12.5mm	9.26nm	
h	3mm	1nm	
k_w		8.99950.35TN/m^3	
k_g		2.071273 N/m	
H_z		2e8 A/m	
V_0		2 volt	
d_0			1.494nm
d_i			1.36nm
e_{31}		-0.13C/m^2	
e_{32}		-0.145 C/m^2	
e_{15}		-0.009 C/m^2	
e_{24}		-0.276 C/m^2	

Table 2
The nonlocal uniaxial and biaxal critical buckling load ratios ($N^{cr} = 12(1-v^2)N_x^{cr}L^2 / c_{11}h^3$) of nanoplate (a/b=1, h=0.34nm, E = 1.06 TPa, K=10 and $v = 0.25$)

The nonlocal parameter ($\mu = e_0 a / L$)	Nonlocal uniaxial critical buckling ratio	Murmu et al. [13]	Nonlocal biaxial critical buckling ratio	Murmu et al. [13]
0	41.5048	41.38000	20.7524	20.85108
0.1	34.8297	33.71278	17.4149	17.30685
0.2	23.6397	23.04766	11.8198	11.5396
0.3	15.5968	15.2744	7.7984	7.65244
0.4	10.7508	10.5488	5.3754	5.21341
0.5	7.8360	7.619771	3.9180	3.91768
0.6	6.0084	6.001938	3.0042	3.00305
0.7	4.8073	4.762199	2.4037	2.39329
0.8	3.9833	3.924212	1.9917	1.938266
0.9	3.3966	3.38736	1.6983	1.710532
1	2.9656	2.92683	1.4828	1.47866

Fig. 2 illustrates the nonlocal biaxial critical buckling load to the local biaxial critical buckling load ratio (λ) of polymeric piezoelectric nanocomposite plate versus aspect ratios of a/b for the different volume fraction of CNT. It is clear that λ decreases with increasing of a/b. As aspect ratio (a/b) increases, the stability of piezoelectric nanocomposite plate reduces, hence λ decreases. Also, λ increases with increasing of the CNT volume fraction.

Effect of elastic foundation parameters on λ of piezoelectric nanocomposite plate is shown in Fig. 3 for different value of the nonlocal parameter. It is obvious that spring and shear constants of the elastic foundation increase stiffness of polymeric piezoelectric nanocomposite plate, thus, this ratio increases. The difference between considering and not considering the elastic foundation is significant for higher nonlocal parameter. On the other hand, the influence of elastic foundation parameters on λ in lower nonlocal parameter is negligible.

Fig. 4 depicts the effect of applied magnetic field on λ versus the nonlocal parameter. It is concluded that λ increases with an increase in the applied magnetic fields. As magnetic fields in *z* direction are applied on polymeric piezoelectric nanocomposite plate, compressive loads are created then λ increases. Also for higher values of the nonlocal parameter, the difference of the various applied magnetic field effect on λ is clear.

Fig. 5 shows the external applied voltage effect on λ of piezoelectric nanocomposite plate for different values of the nonlocal parameter. As it can be seen from this figure, λ increases with considering the external applied voltage. The positive external applied voltage produces compressive load but negative external applied voltage produces tension load. The influence of positive external applied voltage on λ is more than the negative external applied voltage on it.

Effects of external parameters on λ demonstrate in Fig. 6 for the different nonlocal parameter values. In comparison of external parameters, λ of polymeric piezoelectric nanocomposite plate is more affected by elastic foundation, magnetic field in *z* direction and the positive external applied voltage than other parameters, respectively.
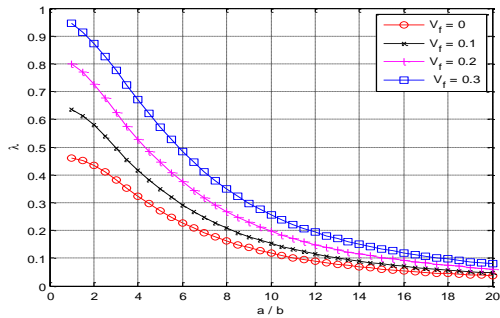

Fig.2
λ of polymeric piezoelectric nanocomposite plate versus aspect ratio (a / b) for various CNT volume fraction.
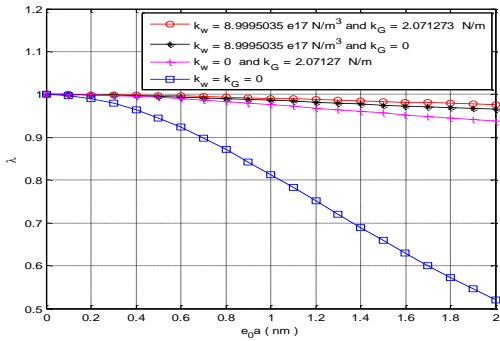

Fig.3
Effects of elastic foundation parameters on λ of polymeric piezoelectric nanocomposite plate for different values of the nonlocal parameter.
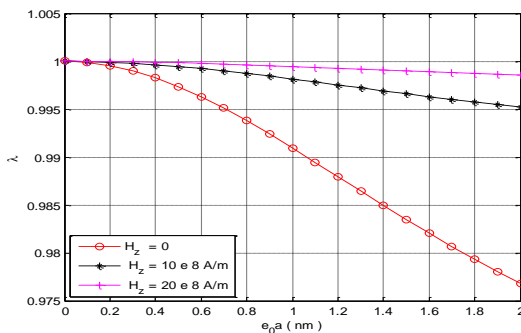

Fig.4
Magnetic field effect on λ of polymeric piezoelectric nanocomposite plate for different nonlocal parameter values.
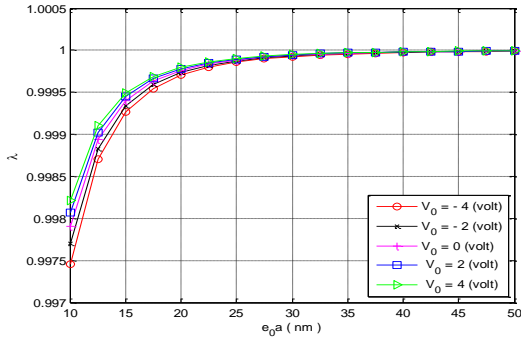
Fig.5
λ of polymeric piezoelectric nanocomposite plate against aspect ratios (b/h) for the different external applied voltage.
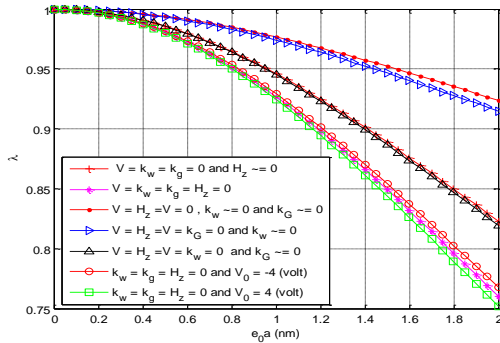

Fig.6
λ of polymeric piezoelectric nanocomposite plate versus the nonlocal parameter for different external parameters.

Figs. 7 and 8 display the effects of nanoplate and CNT residual surface stress constants (τ_s^{plate}, τ_s^{CNT}) on the surface biaxial critical buckling load to the non-surface biaxial critical buckling load ratio (γ) of polymeric piezoelectric nanocomposite plate for different aspect ratios of a/b, respectively. As it can be observed γ decreases with an increase in residual surface stress constant of nanoplate and vice versa in residual surface stress constant of CNT. As residual surface stress produces tension load thus γ decreases. Also, it is noticeable that influence of τ_s^{plate} on γ is higher than the influence of τ_s^{CNT}.

The effects of nanoplate and CNT surface Lame constants (E_s^{plate}, E_s^{CNT}) on γ of piezoelectric nanocomposite plate are illustrated in Figs. 9 and 10 for different aspect ratios of a/b, respectively. It can be seen that the effect of surface Lame constants on γ in larger values of a/b is considerable. Also, the effect of CNT surface parameters on γ of polymeric piezoelectric nanocomposite plate is very lower against the effect of nanoplate surface parameters on this ratio.
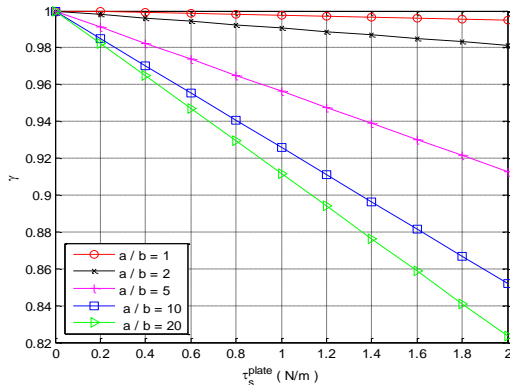

Fig.7
λ against nanoplate residual surface stress constant for different aspect ratio of a/b.
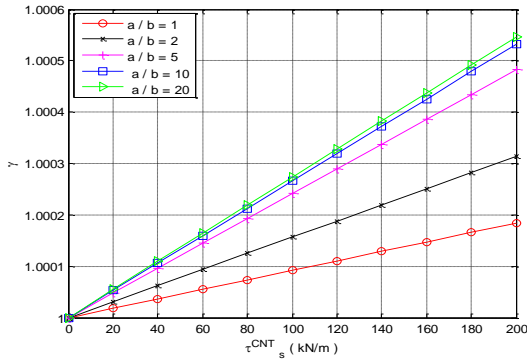
Fig.8
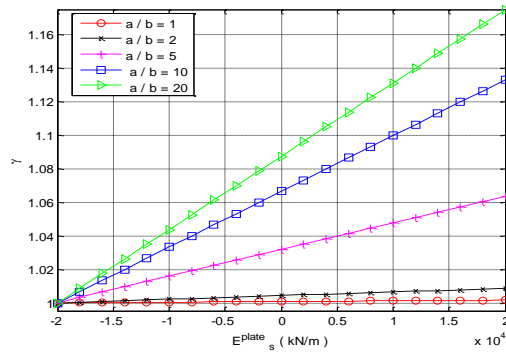λ against CNT residual surface stress constant for different aspect ratio of a/b.

Fig.9
λ with respect to nanoplate surface Lame constant for different aspect ratio of b/h.
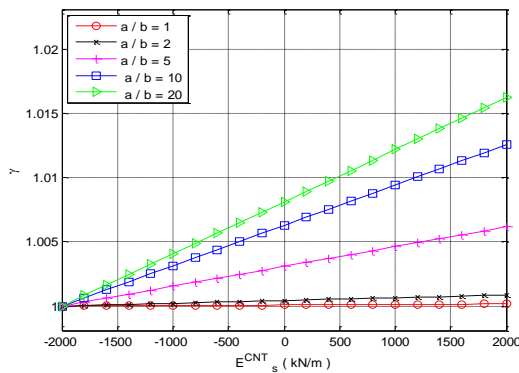

Fig.10
λ against CNT surface Lame constant for different aspect ratio of a/b.

Figs. 11 and 12 depict the effects of τ_s and E_s on γ of piezoelectric nanocomposite plate using CPT and FSDT for the various nonlocal parameter ($e_0 a$), respectively. It can be seen that γ decreases with increasing of τ_s for FSDT and vice versa for CPT and the influence of τ_s on γ becomes lower in higher nonlocal parameter for both plate theories. γ decreases with considering the positive E_s and vice versa with considering the negative E_s. Also the influence of surface Lame constants on γ for both plate theories isn't considerable.

The effects of τ_s and E_s on the nonlocal deflection to local deflection of polymeric piezoelectric nanocomposite plate ratio (η) with respect to the nonlocal parameter for CPT and FSDT are demonstrated in Figs. 13 and 14, respectively. In Fig. 13, it is clear that η decreases with an increase of the nonlocal parameter for both theories. Moreover, for FSDT, η decreases with an increase in τ_s but for CPT, this behavior is inverse. η increases considering the positive E_s and vice versa for the negative E_s. Moreover, E_s has not significant effect on η.
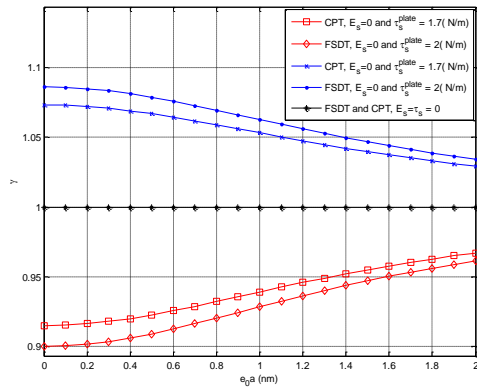
Fig.11
Effect of residual surface stress constant on λ based on CPT and FSDT.
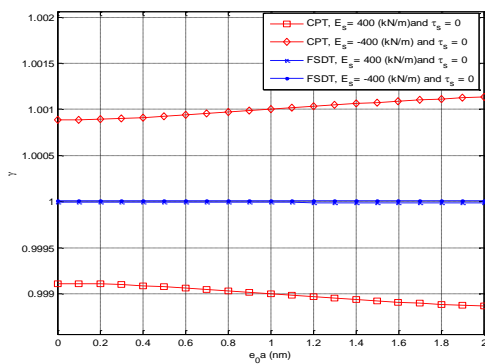

Fig.12
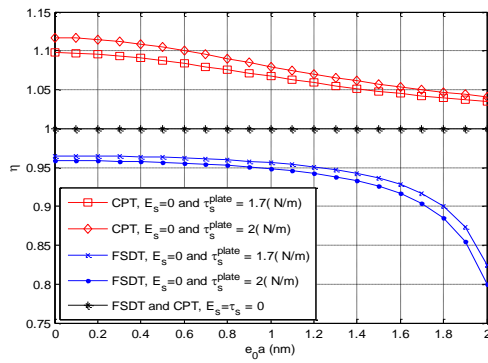Effect of surface Lame constants on λ based on CPT and FSDT.

Fig.13
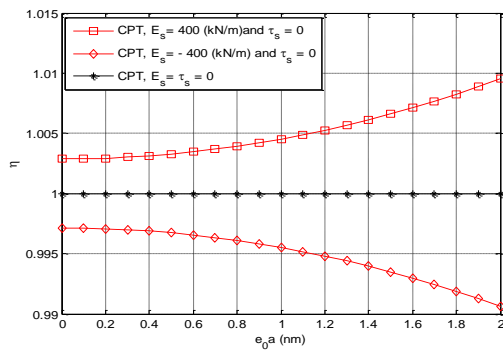Effect of residual surface stress constant on η based on CPT and FSDT.

Fig.14
Effect of surface Lame constants on based on CPT and FSDT.

5 CONCLUSIONS

In this research, the biaxial buckling and bending analysis of polymeric piezoelectric nanoplate reinforced by CNT subjected to electro-magneto-mechanical loadings considering surface effect are studied. Eshelby-Mori-Tanaka approach is used to define piezoelectric nanocomposite plate material properties. Navier's type solution is employed to obtain the biaxial critical buckling load of polymeric piezoelectric nanocomposite plate. Various parameter effects such as: the nonlocal parameter, aspect ratio, CNT volume fraction, surface stress effect parameters, elastic foundation parameters, magnetic field and external applied voltage on the biaxial critical buckling load and bending of piezoelectric nanocomposite plate are investigated. The results of this research are listed as follows:

1. The nonlocal biaxial critical buckling load to the local biaxial critical buckling load ratio (λ) of polymeric piezoelectric nanocomposite plate increases with increase of CNT volume fraction, side to thickness (b/h), elastic foundation parameters, CNT surface Lame constant, the external applied voltage and magnetic fields.
2. λ of polymeric piezoelectric nanocomposite plate decreases with increase of the nonlocal parameter, aspect ratio of a/b, residual surface stress constant and nanoplate surface Lame constant.
3. λ increases with an increase in the external applied voltage, elastic foundation parameters, and magnetic fields.
4. Effects of surface parameter on the surface biaxial critical buckling load to the nonsurface biaxial critical buckling load ratio (γ) of polymeric piezoelectric nanocomposite plate is considerable. γ is more affected by residual surface stress constant of nanoplate than the other surface stress parameters.
5. γ decreases with increase of residual surface stress constant (τ_s).
6. Influence of surface Lame constants on γ and the nonlocal deflection to local deflection of polymeric piezoelectric nanocomposite plate ratio (η) for CPT and FSDT isn't considerable.
7. η decreases with an increase of the nonlocal parameter for both theories.
8. For FSDT, η decreases with an increase in τ_s and vice versa for CPT.

ACKNOWLEDGMENTS

REFERENCES

[1]   Schmidt D., Shah D., Giannelis EP., 2002, New advances in polymer/layered silicate nanocomposites, *Current Opinion in Solid State and Material Science* **6**(3): 205-212.
[2]   Thostenson E., Li C., Chou T., 2005, Review nanocomposites in context, *Journal Composite Science Technology* **65**:491-516.
[3]   Ghorbanpour Arani A., Hashemian M., Loghman A., Mohammadimehr M., 2011, Study of dynamic stability of the double-walled carbon nanotube under axial loading embedded in an elastic medium by the energy method, *Journal of applied mechanics and technical physics* **52** (5): 815-824.
[4]   Mohammadimehr M., Rahmati A. H., 2013, Small scale effect on electro-thermo-mechanical vibration analysis of single-walled boron nitride nanorods under electric excitation, *Turkish Journal of Engineering & Environmental Sciences* **37**: 1-15.
[5]   Ghorbanpour Arani A., Rahnama Mobarakeh M., Shams Sh., Mohammadimehr M., 2012, The effect of CNT volume fraction on the magneto-thermo-electro-mechanical behavior of smart nanocomposite cylinder, *Journal of Mechanical Science and Technology* **26** (8): 2565-2572.
[6]   Jaffe B., Cook W.R., Jaffe H., 1971, *Piezoelectric Ceramics*, New York, Academic.
[7]   Xu S., Yeh Y.W., Poirier G., McAlpine M.C., Register R.A., Yao N., 2013, Flexible piezoelectric PMN-PT nanowire-based na nocomposite and device, *Nano Letters* **13**: 2393-2398.
[8]   Samaei A.T., Abbasion S., Mirsayar M.M., 2011, Buckling analysis of a single-layer graphene sheet embedded in an elastic medium based on nonlocal Mindlin plate theory, *Mechanical Resereach Communication* **38**: 481-485.
[9]   Farajpour A., Shahidi A.R., Mohammadi M., Mahzoon M., 2013, Buckling of orthotropic micro/nanoscale plates under linearly varying in-plane load via nonlocal continuum mechanics, *Composite Structure* **94**: 1605-1615.

[10]   Aksencer T., Aydogdu M., 2011, Levy type solution method for vibration and buckling of nanoplates using nonlocal elasticity theory, *Physica E* **43**: 954-959.

[11]   Narendar S., 2011, Buckling analysis of micro-/nano-scale plates based on two-variable refined plate theory incorporating nonlocal scale effects, *Composite Structure* **93**: 3093-3103.

[12]   Analooei H.R., Azhari M., Heidarpour A., 2013, Elastic buckling and vibration analyses of orthotropic nanoplates using nonlocal continuum mechanics and spline finite strip method, *Appllied Mathematical Modeling* **37**: 6703-6717.

[13]   Murmu T., Sienz J., Adhikari S., Arnold C., 2013, Nonlocal buckling of double-nanoplate-systems under biaxial compression, *Composite Part B* **44**: 84-94.

[14]   Ansari R., Sahmani S., 2013, Prediction of biaxial buckling behavior of single-layered graphene sheets based on nonlocal plate models and molecular dynamics simulations, *Appllied Mathematical Modeling* **37**: 7338-7351.

[15]   Ghorbanpour Arani A., Kolahchi R., Vossough H., 2012, Buckling analysis and smart control of SLGS using elastically coupled PVDF nanoplate based on the nonlocal Mindlin plate theory, *Physica B* **407**: 4458-4465.

[16]   Murmu T., Pradhan S.C., 2009, Buckling of biaxially compressed orthotropic plates at small scales, *Mechanical Research Communication* **36**: 933-938.

[17]   Farajpour A., Danesh M., Mohammadi M., 2011, Buckling analysis of variable thickness nanoplates using nonlocal continuum mechanics, *Physica E* **44**: 719-727.

[18]   Gurtin M.E., Murdoch A.I., 1978, Surface stress in solids, *International Journal of Solids Structure* **14**: 431-440.

[19]   Tian L., Rajapakse R.K.N.D., 2007, Finite element modelling of nanoscale inhomogeneities in an elastic matrix, *Computer Material Science* **41**: 44-53.

[20]   Wang G.F., Feng X.Q., 2009, Timoshenko beam model for buckling and vibration of nanowires with surface effects, *Physics D* **42**: 155-411.

[21]   Wang K.F., Wang B.L., 2013, Effect of surface energy on the non-linear postbuckling behavior of nanoplates, *International Journal of Nonlinear Mechanics* **55**: 19-24.

[22]   Alzahrani E.O., Zenkour A.M., Sobhy M., 2013, Small scale effect on hygro-thermo-mechanical bending of nanoplates embedded in an elastic medium, *Composite Structure* **105**: 163-172.

[23]   Alibeigloo A., 2013, Static analysis of functionally graded carbon nanotube-reinforced composite plate embedded in piezoelectric layers by using theory of elasticity, *Composite Structure* **95**: 612-622.

[24]   Zhu P., Lei Z.X., Liew K.M., 2012, Static and free vibration analyses of carbon nanotube-reinforced composite plates using finite element method with first order shear deformation plate theory, *Composite Structure* **94**: 1450-1460.

[25]   Lei Z.X., Liew K.M., Yu J.L., 2013, Buckling analysis of functionally graded carbon nanotube-reinforced composite plates using the element-free kp-Ritz method, *Composite Structure* **98**: 160-168.

[26]   Jafari Mehrabadi S., Sobhani Aragh B., Khoshkhahesh V., Taherpour A., 2012, Mechanical buckling of rectangular nanocomposite plate reinforced by aligned and straight single-walled carbon nanotubes, *Composite Part B* **43**: 2031-2040.

[27]   Shi D.L., Feng X.Q., huang Y.Y., Hwang K.C., Gao H., 2004, The effect of nanotube waviness and agglomeration on the elastic property of carbon nanotube-reinforced composites, *Journal of Engineering Material Technology* **126**: 250-257.

[28]   Rahmati A.H., Mohammadimehr M., 2014, Vibration analysis of non-uniform and non-homogeneous boron nitride nanorods embedded in an elastic medium under combined loadings using DQM, *Physica B: Condensed Matter* **440**: 88-98.

[29]   Mohammadimehr M., Saidi A. R., Ghorbanpour Arani A., Arefmanesh A., Han Q., 2011, Buckling analysis of double-walled carbon nanotubes embedded in an elastic medium under axial compression using non-local Timoshenko beam theory, *Proceedings of the Institution of Mechanical Engineers, Part C*, *Journal of Mechanical Engineering Science* **225**: 498-506.

[30]   Ansari R., Sahmani S., 2011, Surface stress effects on the free vibration behavior of nanoplates, *International Journal of Engineering Science* **49**: 1204-1215.

[31]   Wang L., 2012, Surface effect on buckling configuration of nanobeams containing internal flowing fluid: A nonlinear analysis, *Physica E* **44**: 808-812.

[32]   Kraus J., 1984, *Electromagnetics*, USA, McGrawHill Inc.

[33]   Ghorbanpour Arani A., Amir S., Shajari A.R., Mozdianfard M.R., Khoddami Maraghi Z., Mohammadimehr M., 2012, Electro-thermal non-local vibration analysis of embedded DWBNNTs, *Proceedings of the Institution of Mechanical Engineers Part C: Journal of Mechanical Engineering Science* **226**: 1410-1422.

[34]   Shen H.S., Zhu Z.H., 2012, Postbuckling of sandwich plates with nanotube-reinforced composite face sheets resting on elastic foundations, *European Journal of Mechanical A/Solids* **35**: 10-21.